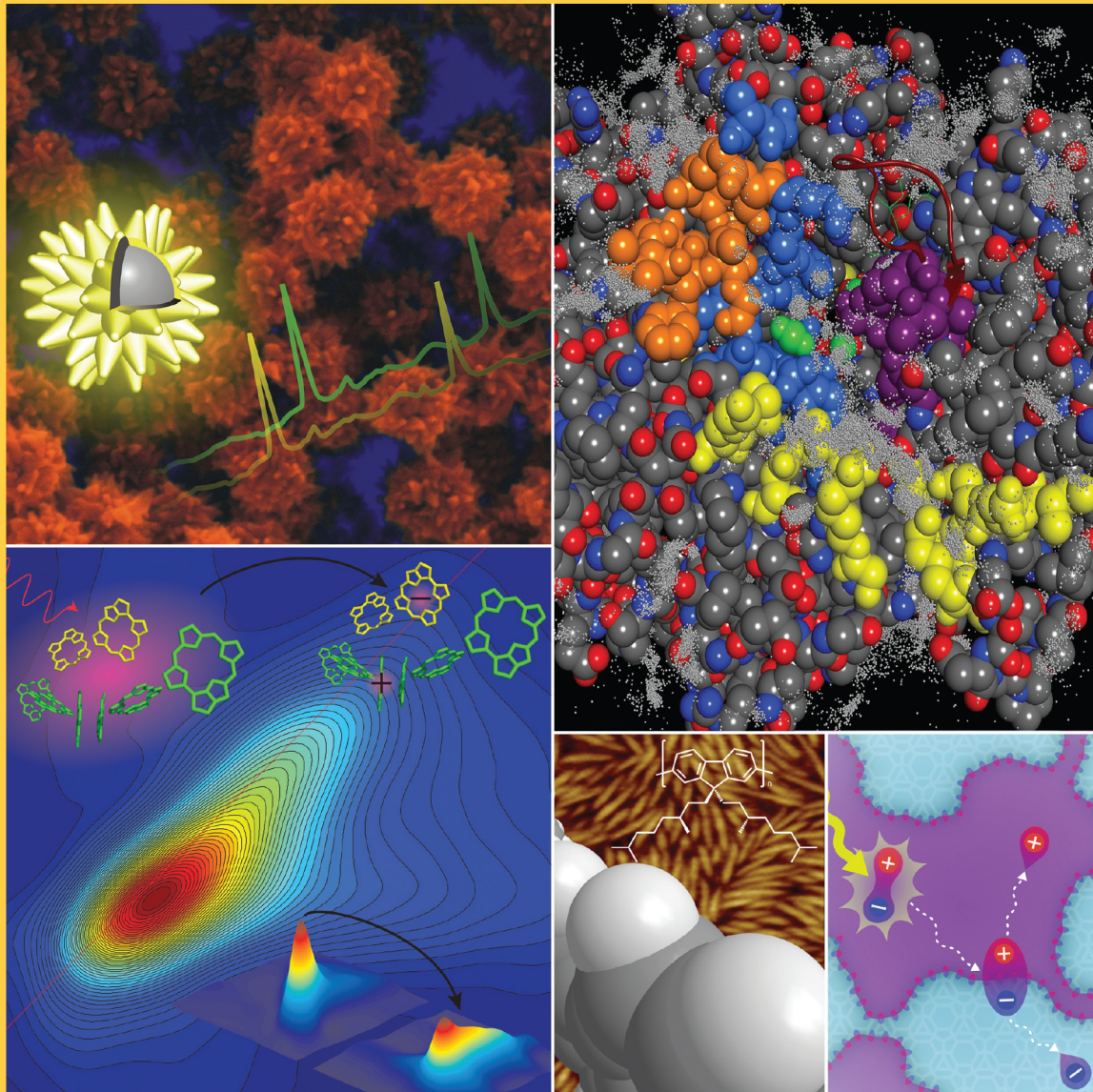


MAY 9, 2013
VOLUME 117
NUMBER 18
pubs.acs.org/JPCB

THE JOURNAL OF PHYSICAL CHEMISTRY B



BIOPHYSICAL CHEMISTRY, BIOMATERIALS, LIQUIDS, AND SOFT MATTER



ACS Publications
MOST TRUSTED. MOST CITED. MOST READ.

www.acs.org

Carbonic Anhydrase Promotes the Absorption Rate of CO₂ in Post-Combustion Processes

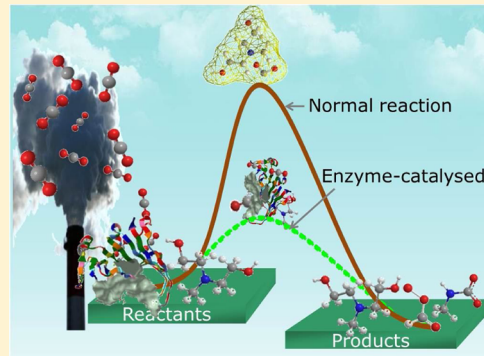
Mari Vinoba,[†] Margandan Bhagyalakshmi,[‡] Andrews Nirmala Grace,[†] Dae Hoon Kim,[†] Yeoil Yoon,[†] Sung Chan Nam,[†] Il Hyun Baek,[†] and Soon Kwan Jeong*,[†]

[†]Korea Institute of Energy Research, Daejeon 305-343, Korea

[‡]CO₂ Research and Green Technologies Centre, VIT University, Vellore- 632014, India

Supporting Information

ABSTRACT: The rate of carbon dioxide (CO₂) absorption by monoethanol amine (MEA), diethanol amine (DEA), *N*-methyl-2,2'-iminodiethanol (MDEA), and 2-amino-2-methyl 1-propanol (AMP) solutions was found to be enhanced by the addition of bovine carbonic anhydrase (CA), has been investigated using a vapor–liquid equilibrium (VLE) device. The enthalpy ($-\Delta H_{\text{abs}}$) of CO₂ absorption and the absorption capacities of aqueous amines were measured in the presence and/or absence of CA enzyme via differential reaction calorimeter (DRC). The reaction temperature (ΔT) under adiabatic conditions was determined based on the DRC analysis. Bicarbonate and carbamate species formation mechanisms were elucidated by ¹H and ¹³C NMR spectral analysis. The overall CO₂ absorption rate (flux) and rate constant (k_{app}) followed the order MEA > DEA > AMP > MDEA in the absence or presence of CA. Hydration of CO₂ by MDEA in the presence of CA directly produced bicarbonate, whereas AMP produced unstable carbamate intermediate, then underwent hydrolytic reaction and converted to bicarbonate. The MDEA > AMP > DEA > MEA reverse ordering of the enhanced CO₂ flux and k_{app} in the presence of CA was due to bicarbonate formation by the tertiary and sterically hindered amines. Thus, CA increased the rate of CO₂ absorption by MDEA by a factor of 3 relative to the rate of absorption by MDEA alone. The thermal effects suggested that CA yielded a higher activity at 40 °C.



1. INTRODUCTION

Since the industrial revolution, large quantities of greenhouse gases (CO₂) have been emitted into the atmosphere, where they have accelerated global warming.^{1–3} In 2011, 33.9 billion tons of CO₂ were discharged from thermoelectric power plants, cement, and steel plants. Large-scale carbon dioxide absorption studies with a potential for high impact have, therefore, focused on these industries.⁴ Postcombustion deposition processes using amine absorbent solvents are highly efficient and selective for capturing CO₂ emitted from coal-fired power plants.⁵ A variety of amine solvents have been identified for CO₂ absorption,⁶ among which the primary amine solvent monoethanolamine (MEA) and secondary amine diethanolamine (DEA) are highly corrosive. The tertiary amine *N*-methyl-2,2'-iminodiethanol (MDEA) is advantageous over the primary and secondary amines in that MDEA displays a low regeneration energy. The stoichiometry of MEA or DEA carbamate/bicarbonate formation suggests that amine could provide a maximum loading capacity of 0.5 mol CO₂/mol amine, whereas the tertiary amine MDEA, which cannot produce carbamate, yields a maximum loading capacity of 1 mol/mol amine. Thus, tertiary amines, such as MDEA, are limited by slow CO₂ reaction rates, although they yield a high CO₂ absorption volume and low corrosion.^{7–9} This study examined the attempts to increase the CO₂ absorption rate of

tertiary MDEA and the sterically hindered amine 2-amino-2-methyl-1-propanol (AMP) solvents. Reports from the literature suggest that the order of CO₂ absorption rate constant was MEA > DEA > AMP > MDEA.¹⁰ Many studies have found that the low CO₂ absorption capacity and rate in amine sorbents can be improved by the addition of certain additives.^{11–15} Several blend compounds, such as piperazine-MDEA, piperazine-AMP, AMP-methylmonoethanolamine, and AMP-morpholine have been identified and mixed with amine solvents to increase the CO₂ absorption rate.^{12,16} Such eutectic amine compound phases display high CO₂ capture; however, the CO₂ capture cost is high.¹⁷ An alternative strategy to blending two amine solvents would be to identify a low-cost solution that yields a high CO₂ absorption rate. This step is crucial to CO₂ capture research.

Recently, it has been proved that enzymatic processes are generally quite rapid compared to other CO₂ sequestration processes.^{18,19} Hence, the biomolecule, carbonic anhydrase (CA) have been attempted to increase the CO₂ absorption rate of the above-discussed amine compounds. CA is a major zinc-based metalloenzyme that catalyzes the conversion of CO₂ to

Received: February 15, 2013

Revised: April 10, 2013

Published: April 15, 2013

bicarbonate or vice versa.²⁰ The proton shuttle histidine-64 residue of CA plays an important role in the hydration reaction that binds in the Zn²⁺-coordinated water or hydroxide center with the carbon of CO₂, and facilitates release of HCO₃⁻. Bovine CA (BCA) increases the CO₂ hydration rate constant to 10⁶ s⁻¹.^{21–23} Recently, CA immobilized on solid supports illustrated excellent yield on CO₂ conversion.^{24–26} Combinations of CA with amine sorbents have not been extensively studied. Hence, the efficiency of combining CA with amine sorbents, such as MEA, DEA, MDEA, or AMP is evaluated based on the enthalpy ($-\Delta H_{\text{abs}}$) of CO₂ absorption, the reaction temperature (ΔT) under adiabatic conditions, and the absorption capacity, as determined by differential reaction calorimeter (DRC). The CO₂ absorption rate and rate constant were obtained using a vapor–liquid equilibrium (VLE) device. The underlying mechanisms of bicarbonate and carbamate formation reactions were elucidated by NMR spectral analysis. In this study, CO₂ absorption rate and heat of absorption were investigated using CA with amine absorbents with an emphasis on the role of CA enhancing the rate.

2. EXPERIMENTAL SECTION

2.1. Materials. The absorbents and enzyme were obtained from Sigma-Aldrich and were used as received: MEA (99.0%), DEA (99.0%), MDEA (99.0%), AMP (95%), and BCA. Aqueous solutions were prepared with 5 wt % or 10 wt % of each of the four amine compounds using Milli-Q water. Ultrapure N₂ (99.999%) and CO₂ (99.999%) gas obtained from Special Gas, Korea, were employed in the VLE device, and 30% CO₂ (balance N₂) gas was used for DRC.

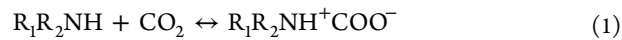
2.2. Vapor–Liquid Equilibrium. The VLE system comprised the gas reservoir, reactor, temperature sensor, pressure gauge, pump, and real-time recorder (Figure S1).²⁷ The total reactor volume was 300 cm³. To the reactor, 150 cm³ amine sorbent (5% or 10%) and the CA enzyme (5 ppm) were added, and stirred magnetically at 300 rpm to carry out the reaction between the absorbent and CO₂. Before introducing the CO₂ into the reactor, the reaction mixture was evacuated using a vacuum pump at room temperature. A water bath was constructed to preheat the reaction mixture and run the reaction at the desired temperature. The reactor was designed in such a way that its internal pressure could be measured during the absorption reactions, and the values could be stored in real time. Absorption tests were performed after opening the connecting valve between the reservoir and the reactor to inject carbon dioxide at a constant pressure. Over the course of the reaction, the pressure in the reactor decreased as a function of the CO₂ absorption. The attainment of absorption equilibrium was determined, when the deviations in the pressure were smaller than 0.001. As a control, the above experiment was carried out in the absence of enzyme. The solutions were characterized by ¹H and ¹³C NMR using a Bruker Avance 500 MHz NMR spectrometer to identify carbamate and bicarbonate species.

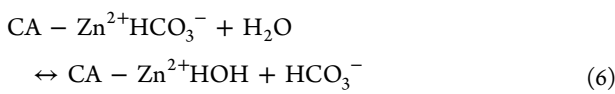
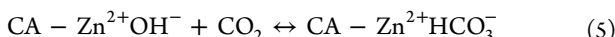
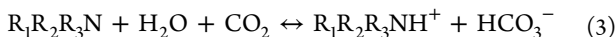
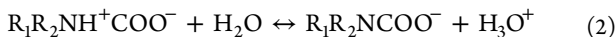
2.3. Differential Reaction Calorimeter. The CO₂ absorption heat and the absorption capacities of the amine solvents were measured using the DRC data (the DRC was manufactured by SETARAM).²⁸ The DRC apparatus consisted of two mechanically agitated glass reactors (250 cm³). The reaction temperature was maintained using a temperature-controlled water bath that was circulated through the reactor and the jacket. The reactor contained a Joule effect calibration probe and thermocouple (± 0.01 °C) for measuring the

reaction temperature (ΔT). The reactor was filled with 100 g of each of the amine solvents (10 wt %) containing the CA enzyme (5 ppm). To enhance contact between the CA enzyme, absorbent, and CO₂, a 30% CO₂ gas mixture (the balance of which was N₂) was supplied in a purge form at 100 mL/min with stirring at 200 rpm. The CO₂ absorption rate and reaction completion were evaluated by analyzing the discharge gas using a TCD detector consisting of a Porapak-Q (2 m, Supelco) column (7890N model GC from Agilent). The experimental temperature was maintained at 40 °C. A control experiment was performed without the enzyme.

3. RESULTS AND DISCUSSION

3.1. CO₂ Absorption by the Equilibrium Method. The reactions between carbon dioxide and various amine absorbents, such as MEA (primary amine), DEA (secondary amine), MDEA (tertiary amine), or AMP (hindered amine) in aqueous solutions (5 wt % and 10 wt %) were studied at 10, 25, 40, 50, and 60 °C. Absorption of CO₂ in the amines involved passing CO₂ gas through an aqueous amine solution until equilibrium had been reached. The plausible mechanism for products formation by CO₂+amine+H₂O systems is enumerated through the eqs 1–6. The aqueous primary (MEA) and secondary (DEA) amine produced amine carbamates and bicarbonates, primarily in their ionic forms, via acid–base interactions through a zwitterion intermediate.²⁹ The zwitterion mechanism involved a two-step process: initially a carbamate formed during CO₂ absorption by the first amine group, the intermediate subsequently formed hydrogen bonds with a nearby nitrogen atom of a second amine group, thereby stabilizing the chemisorbed CO₂ and producing bicarbonate. Here, the amines acted as a base, reacting with the carbonic acid formed from the dissolution of CO₂ in water (eq 1–2). The above equation shows that the CO₂ reaction ratio with MEA ($R_1 = \text{CH}_2\text{CH}_2\text{OH}$, $R_2 = \text{H}$) and DEA ($R_1 = (\text{CH}_2\text{CH}_2\text{OH})_2$, $R_2 = \text{H}$) was 0.5 mol CO₂/mol amine. The tertiary amine MDEA ($R_1 = R_2 = \text{CH}_2\text{CH}_2\text{OH}$, $R_3 = \text{CH}_3$) did not produce carbamates via direct reaction with CO₂ because they had no hydrogen atoms bound to the nitrogen; instead, tertiary amines formed a protonated amine and a hydroxyl ion in aqueous solutions. The OH⁻ produced reacted with CO₂ to produce bicarbonate (eq 3).^{30,31} The sterically hindered amine AMP ($R = \text{C}(\text{CH}_3)_2\text{CH}_2\text{OH}$) produced carbamate at the amino group, which was attached to a tertiary carbon atom. Substituent groups can affect the donating or withdrawal of electrons via steric hindrance effects. The carbamates produced by AMP were unstable; therefore a hydrolytic reaction occurred, converting the carbamate to a bicarbonate (eq 4).³¹ Equations 3 and 4 show that the CO₂ capture efficiency of MDEA and AMP was 1 mol CO₂/mol amine. Overall, the CO₂ absorption reaction of MDEA and AMP proceeded in a single-step mechanism. CA is a zinc metalloenzyme that catalyzes the interconversion of CO₂ and bicarbonate (eq 5–6). A zinc-bound water molecule in CA is ionized to a Zn–OH⁻ ion that attacks the carbon of CO₂.²⁵ The active enzyme is subsequently regenerated through intermolecular H⁺ transfer between the CA and H⁺ acceptor amine molecules. CA is an effective promoter of CO₂ absorption in amine solvents. The underlying mechanism for this reaction was elucidated using NMR spectroscopy.





The carbamate formation mechanism was revealed by NMR data. Figures 1 and 2 show the ^{13}C NMR and ^1H NMR of the

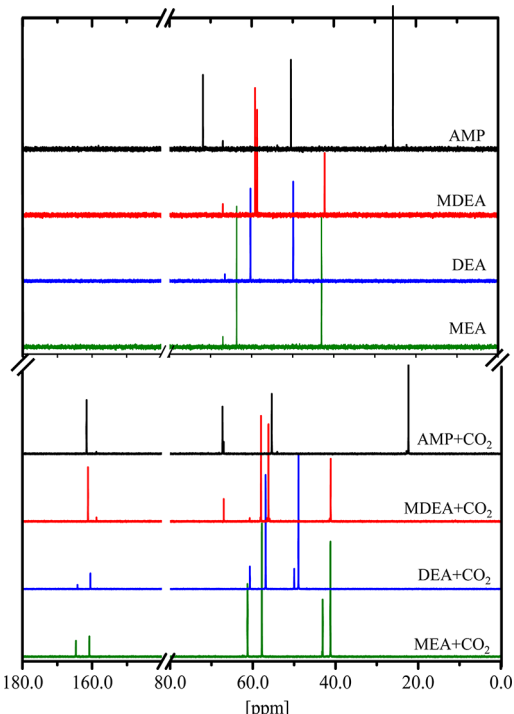


Figure 1. ^{13}C NMR spectra of the pristine and CO_2 -absorbed alkanolamines.

various pristine amine sorbents (MEA, DEA, MDEA, and AMP) and the CO_2 -absorbed amines prepared in the presence of CA enzyme. The chemical shifts of the carbon atoms (from the ^{13}C NMR spectra) and the protons (from the ^1H NMR spectra) with or without CO_2 -absorbed amine sorbents are listed in Table 1. The ^1H NMR spectrum of the CO_2 -absorbed MEA showed a triplet signal at $\delta = 3.56$ ppm and two overlapping triplets at $\delta = 3.11$ ppm, corresponding to the methylene protons at the α -position with respect to the oxygen atoms and nitrogen atoms of the carbamate ion ($[\text{HOCH}_2\text{CH}_2\text{NHCO}_2^-][^+\text{H}_3\text{NCH}_2\text{CH}_2\text{OH}]$). Similarly, the CO_2 -absorbed DEA also yielded signals at $\delta = 3.65$ and $\delta = 3.35$ ppm, corresponding to the above-described species formation. The ^{13}C NMR spectra of MEA and DEA after CO_2 absorption revealed the formation of bicarbonate and carbamate species through the chemical shifts $\delta = 160$ ppm and $\delta = 164$ ppm, respectively,^{32,33} providing evidence that the amine reacted as described in eqs 1 or 2 toward CO_2 absorption. MDEA and AMP reacted with CO_2 to exclusively produce bicarbonate, as verified by a single peak at $\delta = 161$ ppm, shown in Figure 1.^{34,35} These results supported the conclusion that MDEA and AMP

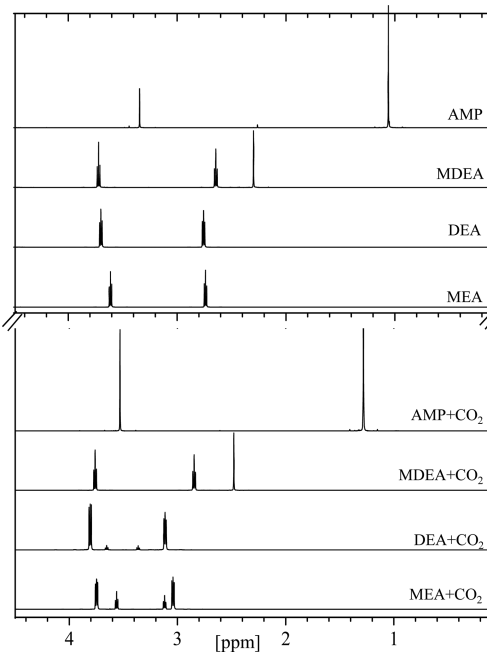


Figure 2. ^1H NMR spectra of the pristine and CO_2 -absorbed alkanolamines.

reacted according to eqs 3 and 4 during the CO_2 absorption processes. All alkanolamines reacted with CO_2 , and the ^{13}C NMR spectra revealed peaks associated with $\text{HCO}_3^-/\text{CO}_3^{2-}$ species at $\delta = 160.5$ – 161.5 ppm. These peaks are barely visible in Figure 1 because of the intensity of the main peak. It was not possible to distinguish between HCO_3^- and CO_3^{2-} due to the rapid exchange of protons between the amines and the protonated amines. A single peak in the spectrum may represent both HCO_3^- and CO_3^{2-} or both the amine and amine– H^+ , as shown in Figure 1. Thus, the species identified by NMR support the mechanism for CO_2 absorption as described above.

The mechanism underlying CO_2 absorption was further investigated by thermodynamic equilibrium data for the amine– CO_2 systems, using apparent equilibrium constants based on species concentrations and representing the reactions in the $\text{CO}_2 + \text{amine} + \text{H}_2\text{O}$ systems.^{36–39} Figure 3 describes the CO_2 absorption in the VLE system in the presence of 5% or 10% aqueous MEA, DEA, MDEA, or AMP and without the CA enzyme, at 10, 25, 40, 50, or 60 °C. The CO_2 absorption was monitored by measuring the equilibrium partial pressure of CO_2 , which decreased as the temperature increased. The CO_2 flux could be determined from the CO_2 partial pressure. The CO_2 flux into the amine solvent was directly proportional to the CO_2 driving force between the partial pressure of CO_2 in the gas phase and the equilibrium partial pressure of CO_2 exerted by the solvent. The flux and apparent rate constant (k_{app}) are defined according to the following equation:

$$\text{flux} = \frac{k_{\text{app}} \times C_{\text{CO}_2}}{RT}$$

Here, C_{CO_2} is the difference between the initial and final equilibrium concentrations of CO_2 in the solution. k_{app} indicates the apparent velocity constant (min^{-1}) with respect to the time and amine concentration, as the partial pressure of CO_2 decreased under equilibrium conditions. T is the reaction temperature, and R is the ideal gas constant.

Table 1. Chemical Shifts of the ^1H NMR and ^{13}C NMR Spectra for Pristine and CO_2 Absorption by the 10% Aqueous Alkanolamine Solutions

MEA+ CO_2	$-\text{CH}_2\text{OH}$	$-\text{CH}_2\text{NH}_2$	$-\text{CH}_2\text{NHCO}_2^-$	$\text{HOCH}_2\text{CH}_2\text{NHCO}_2^-$	HCO_3^-	CO_2^{2-}
MEA	63.62 (3.61)	42.98 (2.73)	-	-	-	-
MEA+ CO_2	61.25 (3.72)	41.23 (3.04)	43.23 (3.11)	57.77 (3.56)	160.80	164.69
DEA+ CO_2	$-\text{CH}_2\text{OH}$	$(-\text{CH}_2)_2\text{NH}$	$(-\text{CH}_2)_2\text{NCO}_2^-$	$(\text{HOCH}_2\text{CH}_2)_2\text{NCO}_2^-$	HCO_3^-	CO_2^{2-}
DEA	60.78 (3.70)	50.38 (2.75)	-	-	-	-
DEA+ CO_2	60.69 (3.70)	48.97 (3.09)	49.98 (3.35)	56.71 (3.65)	160.54	164.18
MDEA+ CO_2	$-\text{CH}_2\text{OH}$	$-\text{NCH}_3$	-	$(\text{HOCH}_2\text{CH}_2)_2\text{NCH}_3$	HCO_3^-	CO_2^{2-}
MDEA	58.65 (3.72)	42.21 (2.29)	-	59.12 (2.64)	-	-
MDEA+ CO_2	56.02 (3.78)	41.16 (2.51)	-	58.02 (2.87)	161.58	-
AMP+ CO_2	$-\text{CH}_2\text{OH}$	$-\text{NC}(\text{CH}_3)_2$	-	$\text{HOCH}_2(\text{CH}_3)_2\text{CNH}_2$	HCO_3^-	CO_2^{2-}
AMP	67.0 (3.34)	25.58 (1.06)	-	50.39	-	-
AMP+ CO_2	67.31 (3.53)	22.35 (1.27)	-	55.41	161.58	-

The values indicate the chemical shifts of the ^{13}C NMR and ^1H NMR spectra (within parentheses).

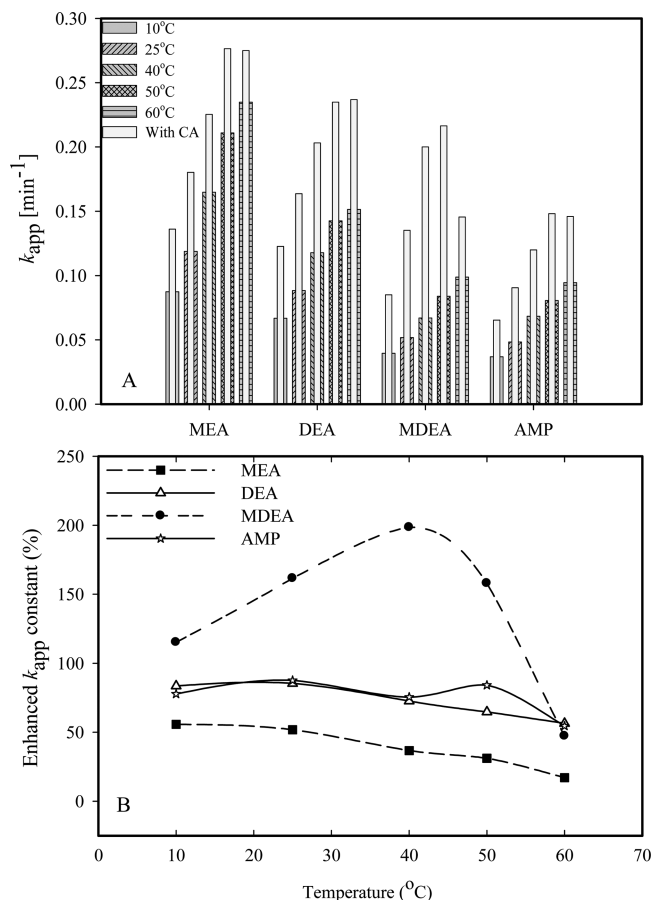


Figure 3. Optimization of the temperature that maximized the CO_2 absorption rate (A), and enhanced rate (B) by the presence of the CA enzyme in 5% of alkanolamines.

Figure 3 shows that the apparent rate constant (k_{app}) was directly proportional to the temperature for all four amine sorbents, in both the absence and presence of CA, irrespective of the amine solvent concentration (5% or 10%). All pure amine absorbents showed a maximum k_{app} at 60 °C, and a 5%

aqueous MEA, DEA, MDEA, or AMP exhibited a 2.68, 2.26, 2.50, or 2.56-fold higher CO_2 absorption rate at 60 °C than at 10 °C. The order of the maximum absorption rate was as follows: MEA > DEA > MDEA > AMP at 60 °C. The apparent rate constant in the presence of the enzyme at 10, 25, 40, 50, or 60 °C revealed that the activity of the CA enzyme increased with temperature up to 50 °C, because its activity depends on temperature, and the biomimetic hydration of CO_2 into bicarbonates occurred at 40 °C.⁴⁰ A minor deviation was observed for the activity of the CA enzyme between 40 and 50 °C (Figure 3B), which might be due to the denaturation of CA.^{41,42} Hence it is observed that CA enzyme improved the apparent rate constant and achieved a high loading capacity at low temperatures (40 °C). Furthermore, the enhanced k_{app} (%) was calculated for aqueous amine sorbents with respect to control reaction by the following equation:

$$\text{Enhanced } k_{\text{app}} (\%) = \frac{(E_{\text{kapp}} - C_{\text{kapp}}) \times 100}{C_{\text{kapp}}}$$

Here, E_{kapp} is the overall absorption apparent rate constant of enzyme based system (Enzyme+absorbent) and C_{kapp} is the overall absorption apparent rate constant of control (pristine absorbent) system.

The enhanced k_{app} (%) values of 5% aqueous MEA, DEA, AMP, or MDEA solutions, calculated from the VLE data in the presence of CA, were 36, 72, 75, or 198% with respect to the control at 40 °C, and the enhanced CO_2 absorption rate order was reverse, i.e., MDEA > AMP > DEA > MEA. Indeed, as a biocatalyst, the enzyme CA may be ignored in view of the thermodynamic stabilities of the carbon dioxide, carbonate/bicarbonate, and carbamate systems; however, the introduction of the enzyme accelerated the rate of CO_2 absorption, possibly due to the intermolecular transfer of protons from the enzyme to the amine, as is observed in the salting in/out effects in $\text{CO}_2+\text{amine}+\text{H}_2\text{O}$ systems.⁴³

The MEA, DEA, and AMP amines were involved in CO_2 absorption via carbamate formation, followed by bicarbonate, whereas, MDEA directly produced bicarbonate via a favorable intermolecular proton transfer. The k_{app} values were higher for

the solvent with higher amine content (10%) than for the 5% amine solvent (Figure S2A). The maximum enhanced CO_2 absorption rate constant by BCA at 40 °C for MEA, DEA, AMP, and MDEA were 0.05, 0.12, 0.16, and 0.20 min⁻¹, respectively. The CA enzyme (5 ppm) showed an enhanced absorption rate, by about 190%, by solutions having either MDEA amine concentration (5% or 10%) relative to the control (Figure 3B or S2B).

The above discussion may be understood in terms of the correlation between the partial pressure versus time and the CO_2 flux versus the partial pressure, for both the 5% and 10% amine sorbent solutions in the presence or absence of CA, as shown in Figures 4A,B and S3 (Supporting Information),

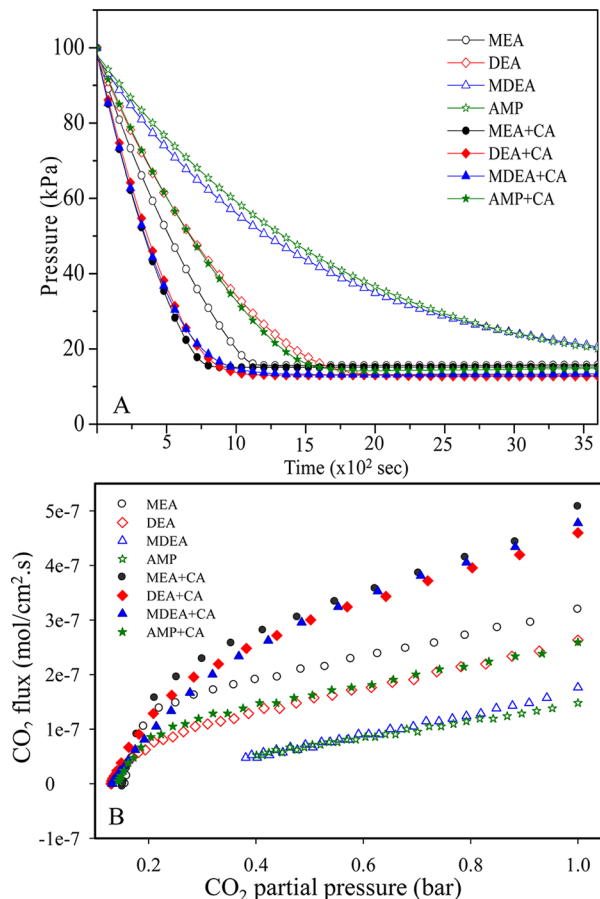


Figure 4. Reaction rate for the absorption of CO_2 by the 5% aqueous amine solutions at 40 °C (A), and the CO_2 driving force for the gas–solvent system in the presence of the CA enzyme (B).

respectively. Figure 4A shows a clear pressure difference between the slow absorption rates of MDEA or AMP and those of MEA and DEA in control experiments. By contrast, in the presence of the CA enzyme, the degree of increasing absorption rate of MDEA was very high compared to that of the other absorbents due to the formation of a bicarbonate species. Here, CA provided the dual function of promoter and catalyst for the hydration of CO_2 .^{18,43} The flux of CO_2 into the absorbents was calculated from the partial pressures of CO_2 in the gas and liquid phases. Figure 4B shows the CO_2 absorption velocities of the CO_2 absorbent systems, revealing that CA enhanced the rate of CO_2 absorption relative to the control experiment. Similarly, in a 10% aqueous amine solution, Figure S3A implies that the pressure decreases with time in the following order

MEA > DEA > AMP > MDEA in the absence of CA, whereas in CA, the enhanced order is MDEA > AMP > DEA > MEA (which is determined by the difference in pressure drop between the amine system with CA and control). The observed revised order is due to rapid decrease in pressure for the amine system in the presence of CA; here CA accelerates the rate of CO_2 absorption of alkanolamines. Further, this pressure drop is used to calculate the CO_2 flux for amine compounds. Thus, from Figure S3B, it is revealed that the amine compounds in the presence of CA has higher flux rates than control system, which might be due to the CO_2 drive force at gas–liquid interface lessening with time. It is also inferred from the figure that the flux rate difference for MDEA with and without enzyme was higher than the other amine system. Hence the flux rate difference between amine system with CA and its enzymeless counterpart (control) order is MDEA > AMP > DEA > MEA. These results indicate that both the nature of the amine sorbent and the concentration of the amine sorbent influence the partial pressure drop and the CO_2 absorption flux, whereas the addition of CA predominately controlled and enhanced the apparent rate constant (k_{app}) for the CO_2 absorption process. Furthermore, CO_2 absorption process at dilute 5% or 10% of amine–water systems (~0.04 M – 0.16 M), the denaturation of BCA is negligible, and hence the catalytic activity is due to the original form of BCA, because the tertiary structure of BCA is maintained at temperature between 25 and 40 °C,⁴¹ and the hydration activity also showed high at pH 10.5 with trimethylamine or carbonate medium.⁴⁴ These alkanolamines are weak bases with pK_a values 9.50, 8.80, 8.57, and 9.82 for MEA, DEA, MDEA and AMP, respectively.¹⁰ According to the literature,⁴² denatured BCA was used for CO_2 absorption experiments (control) with and without absorbent and results showed that, in both the cases, similar k_{app} values with $\pm 5\%$ deviation was observed. These results showed that use of denatured BCA is comparable to reactions without CA. Thus denatured CA has no activity for CO_2 absorption process, and hence the catalytic activity is due to the original form of BCA. Also, no denaturation of fold of BCA occurs under this condition, viz., temperature (40 °C).⁴⁵

3.2. Heat of Reaction by Calorimeter Method. The heat of the reaction for the amine absorbents was measured using a DRC system. The system functions by measuring the differential thermal analysis, determined by the difference between the temperatures of a reference reactor and a sample reactor. The quantity of absorbed CO_2 was obtained by an indirect method, and unreacted CO_2 was quantified using gas chromatography coupled with a thermal conductivity detector. The quantity of heat produced during a reaction could be calculated from the area of integration of the exothermic peak measured after Joule effect calibration before or after the reaction using the SETARAM software. This calibration enabled determination of the product of the reactor's exchange area based on the thermal exchange coefficient (UA). The heat exchanged between the reaction mixture and the reactor wall was proportional to the area under the curve corresponding to ΔT as a function of time. The temperature difference between the two reactors was recorded as a function of time. The following equations are useful for calculating the quantity of heat, heat of absorption, and temperature increase:^{46,47}

$$Q = UA \times S$$

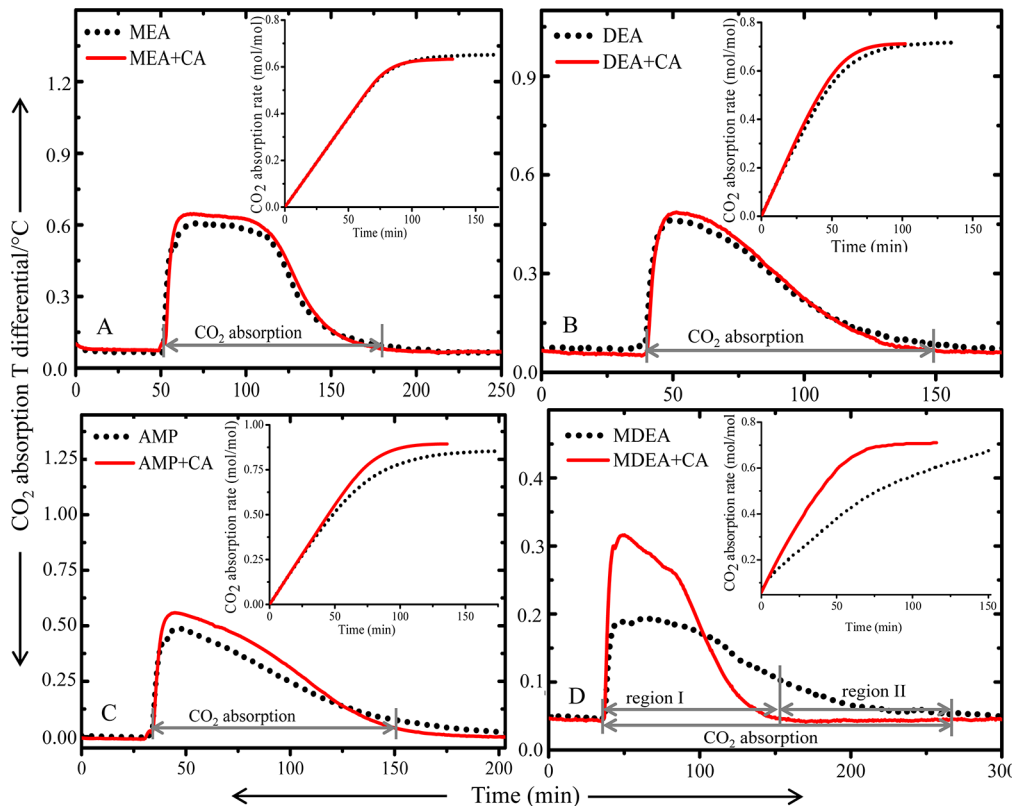


Figure 5. DRC curves for the reaction heat flow during CO_2 absorption by MEA (A), DEA (B), AMP (C), and MDEA (D) at 40 °C with or without the CA enzyme. The inset shows the CO_2 absorption rate determined by gas chromatography.

$$\Delta H = \frac{Q}{m} \times 10^{-3}$$

$$\Delta T = \frac{Q}{C_p \times M}$$

where Q is the quantity of heat released during CO_2 absorption (J), S is the area of integration of the exothermic peak ($^{\circ}\text{C}\cdot\text{s}$), m is the number of moles of CO_2 absorbed, ΔH is the heat of absorption per mole CO_2 (kJ mol^{-1}), C_p is the heat capacity of the absorbent ($\text{J g}^{-1} \text{K}^{-1}$), M is the total mass of the reagents (g), and ΔT is the temperature increase under adiabatic conditions ($^{\circ}\text{C}$).

Figure 5 shows the CO_2 absorption rate and heats of absorption for the MEA, DEA, AMP, and MDEA at 40 °C. During CO_2 absorption, both MEA and DEA solutions produced carbamate and bicarbonate via the zwitterion mechanism. The CA enzyme altered the CO_2 absorption rate by aqueous MEA and DEA, which involved two steps (eqs 1 and 2). Water molecules acted as a base, and the undesirable carbamate formation proceeded, decreasing the absorption capacity and releasing larger quantities of heat ($-\Delta H_{\text{abs}}$). The MEA absorption process took longer to complete due to carbamate anion formation (Figure 5A). MEA had a lower absorption capacity and a higher absorption heat compared to DEA (Figure 5B), as the carbamate formation proceeded to a lesser extent than in MEA. Secondary amines favor the formation of bicarbonate anions because a neighboring DEA molecule can be involved in zwitterion stabilization, thereby shortening the reaction process. The absorption capacities of MEA were 0.63 and 0.65, and for DEA, 0.71 and 0.72 mol/mol CO_2 in the absence and presence of CA enzyme, respectively.

The absorption heat capacities followed the reverse trend because MEA produced more carbamate anions than DEA. After initiation of the absorption process, the absorption heat difference between the sample and the reference decreased slowly. The heat of absorption ($-\Delta H_{\text{abs}}$) and the absorption capacity calculated from Figures 5 is listed in Table 2 for all four

Table 2. CO_2 Absorption Capacity and Heat of Reaction at 40°C

absorbents (10%)	CO_2 loading (mol/mol)	Q (-kJ)	ΔH (-kJ/ mol of CO_2)	ΔT (°C)
MEA	0.63 (0.65)	8.33 (8.89)	80 (88)	20.87 (22.30)
DEA	0.71 (0.72)	4.26 (4.46)	63 (66)	10.58 (11.08)
MDEA	0.69 (0.70)	3.40 (3.32)	58 (56)	8.14 (8.25)
AMP	0.85 (0.89)	7.18 (7.66)	77 (78)	13.91 (18.11)

The values in parentheses indicate the absorbents with the CA enzyme. The values were presented as the average of triplicate analysis (error <4%).

amine sorbents in the absence and presence of CA. The enthalpy values of MEA and DEA were high in the presence of CA enzyme due to enhanced CO_2 absorption rate, and hydration in the aqueous medium and the conversion to bicarbonate.

Significantly, MEA and AMP are both classified as primary amines, but they are engaged in different CO_2 absorption mechanisms. AMP generated carbamates, but the alkyl group attached to the carbon close to the amine group produced steric hindrance and hence the unstable carbamate to bicarbonate conversion is more feasible. This causes an enhanced heat of reaction in AMP than MEA. The CA enzyme

favored conversion of the aqueous CO₂ to bicarbonate. CA increased the CO₂ absorption rate and increased the heat capacity in AMP (Figure 5C). A large quantity of heat was released during the conversion of carbamate to bicarbonate because AMP mainly absorbed CO₂ as a bicarbonate anion from the unstable carbamates. The CO₂ loading and enthalpy ($-\Delta H_{abs}$) of AMP were 0.85, 0.89 mol/mol CO₂, and 77, 78 kJ/mol CO₂ in the absence and presence of the CA enzyme, respectively (Table 2).

The tertiary alkanolamine (MDEA) thus provided a higher degree of CO₂ absorption. The relatively lower rate of absorption in MDEA solvents could be increased by the addition of the CA enzyme. MDEA did not directly react with CO₂ to form carbamates; rather, MDEA acted as a base to form a hydrogen bond between MDEA and water, thereby weakening the hydroxyl bond in water and increasing the reactivity toward CO₂ in solution to form bicarbonates. This reaction proceeded via the base-catalyzed hydration of CO₂. The CA enzyme and MDEA acted by the same mechanism. CA contains a Zn-bounded OH⁻ moiety, which reacted with CO₂ to form bicarbonate. In the presence of CA, the CO₂ absorption rate and loading increased and, at the same time, the heat of absorption decreased because the only product was bicarbonate (not carbamate, Figure 5D). The absorption capacities of MDEA based in region-I, and II were 0.62, 0.70 and 0.69, 0.70 mol/mol CO₂ in the absence and presence of CA, respectively. In region I, it can be clearly seen that the presence of CA enzyme accelerates the rate of absorption to reach equilibrium at a shorter period, whereas control reaction revealed a lengthier period for completion of reaction (region II, Figure 5D). The CO₂ absorption enthalpies and temperature difference were 58, 56 kJ/mol CO₂ and 8.14, 8.25 °C in the absence and presence of CA, respectively. The CO₂ loading and the heat of reaction for the conventional amines followed the order AMP > DEA, MDEA >MEA, and MEA > AMP > DEA > MDEA, respectively. Table 2 shows that the temperature increases in the conventional amine solutions during CO₂ absorption under adiabatic conditions (ΔT) following the trend MEA > AMP > DEA > MDEA. Among the four alkanolamines, the CA enzyme enhanced the CO₂ absorption rate, and decreased the quantity of heat and enthalpy of MDEA. Hence, MDEA is a suitable solvent for industrial CO₂ absorption processes because of its low enthalpy, low heat of reaction, and cost effectiveness.

4. CONCLUSIONS

The carbon dioxide (CO₂) absorption rates of the MEA, DEA, MDEA, and AMP absorbents were enhanced in the presence of BCA. The CO₂ absorption rate (flux) and rate constant (k_{app}) were calculated from VLE measurements, which monitored the partial pressure of CO₂. The correlation between the partial pressure versus time and the CO₂ flux versus partial pressure for both the 5% and 10% amine absorbents in the presence or absence of CA showed that the partial pressure drop and flux for CO₂ absorption followed the order MDEA > AMP > DEA > MEA in the presence of CA and MEA > DEA > AMP > MDEA in the absence of CA, thereby demonstrating that CA enhanced k_{app} . The reverse order of the CO₂ absorption rate in the presence of CA was due to bicarbonate formation by the tertiary and sterically hindered amines. A plausible mechanism was proposed and verified through the capture of carbamate species through ¹³C NMR and ¹H NMR spectral analysis. The heat of reaction for the amine absorbents was measured using a

DRC system. The heat of absorption for MDEA was 58, 56 kJ/mol CO₂ in the absence or presence of CA, respectively. These results were comparatively better than the values obtained for MEA, DEA, and AMP. A high CO₂ absorption rate and a low enthalpy are threshold criteria for the industrial use of CO₂ sequestration processes. The tertiary amine sorbent MDEA was found to satisfy these requirements in the presence of CA. The other amine sorbents may also be used in industrial sequestration, where the large amount of heat dissipated may be utilized for steam generation. In summary, the addition of a green biocatalyst CA increased the CO₂ absorption rate in alkanolamines to yield good CO₂ loading.

■ ASSOCIATED CONTENT

S Supporting Information

Additional figures. This material is available free of charge via the Internet at <http://pubs.acs.org>.

■ AUTHOR INFORMATION

Corresponding Author

*Mailing address: Climate Change Technology Research Division, Korea Institute of Energy Research, 102 Gajeong-ro, Yuseong-gu, Daejeon 305-343, Korea. Fax: (+82) 42-860-3134. E-mail: jeongsk@kier.re.kr.

Notes

The authors declare no competing financial interest.

■ ACKNOWLEDGMENTS

This work was supported by the Korea CCS R&D Center (KCRC) with a grant funded by the Korean Government (Ministry of Education, Science and Technology) (No. 2012-0008933).

■ REFERENCES

- (1) Edenhofer, O.; Pichs-Madruga, R.; Sokona, Y.; Seyboth, K.; Matschoss, P.; Kadner, S.; Zwickel, T.; Eickemeier, P.; Hansen, G.; Schlömer, S.; Von Stechow, C. *IPCC Special Report on Renewable Energy Sources and Climate Change Mitigation*; Cambridge University Press: New York, 2012.
- (2) Shakun, J. D.; Clark, P. U.; He, F.; Marcott, S. A.; Mix, A. C.; Liu, Z.; Otto-Bliesner, B.; Schmittner, A.; Bard, E. Global warming preceded by increasing carbon dioxide concentrations during the last deglaciation. *Nature* **2012**, *484*, 49–54.
- (3) Desideri, U.; Paolucci, A. Performance modelling of a carbon dioxide removal system for power plants. *Energy Convers. Manage.* **1999**, *40*, 1899–1915.
- (4) Olivier, J. G. J.; Janssens-Maenhout, G.; Peters, J. A. H. W. *Trends in Global CO₂ Emissions 2012 Report*; PBL Publishers: Netherlands, 2012.
- (5) Rochelle, G. T. Amine scrubbing for CO₂ capture. *Science* **2009**, *325*, 1652–1654.
- (6) Puxty, G.; Rowland, R.; Allport, A.; Yang, Q.; Bown, M.; Burns, R.; Maeder, M.; Attalla, M. Carbon dioxide post combustion capture: A novel screening study of the carbon dioxide absorption performance of 76 amines. *Environ. Sci. Technol.* **2009**, *43*, 6427–6433.
- (7) Kim, I.; Svendsen, H. F. Comparative study of the heats of absorption of post-combustion CO₂ absorbents. *Int. J. Greenhouse Gas Control* **2010**, *5*, 390–395.
- (8) Aroua, M. K.; Haji-Sulaiman, M. Z.; Ramasamy, K. Modelling of carbon dioxide absorption in aqueous solutions of AMP and MDEA and their blends using Aspenplus. *Sep. Purif. Technol.* **2002**, *29*, 153–162.
- (9) Amann, J. M. G.; Bouallou, C. Kinetics of the absorption of CO₂ in aqueous solutions of *N*-methyl diethanolamine plus triethylene tetramine. *Ind. Eng. Chem. Res.* **2009**, *48*, 3761–3770.

- (10) Vaidya, P. D.; Kenig, E. Y. CO₂-alkanolamine reaction kinetics: A review of recent studies. *Chem. Eng. Technol.* **2007**, *30*, 1467–1474.
- (11) Farmahini, A. H.; Kvamme, B.; Kuznetsova, T. Molecular dynamics simulation studies of absorption in piperazine activated MDEA solution. *Phys. Chem. Chem. Phys.* **2011**, *13*, 13070–13081.
- (12) Barzaghi, F.; Mani, F.; Peruzzini, M. Continuous cycles of CO₂ absorption and amine regeneration with aqueous alkanolamines: A comparison of the efficiency between pure and blended DEA, MDEA and AMP solutions by ¹³C NMR spectroscopy. *Energy Environ. Sci.* **2010**, *3*, 772–779.
- (13) Dubois, L.; Thomas, D. Screening of aqueous amine-based solvents for post combustion CO₂ capture by chemical absorption. *Chem. Eng. Technol.* **2012**, *35*, S13–S24.
- (14) Samanta, A.; Bandyopadhyay, S. S. Absorption of carbon dioxide into aqueous solutions of piperazine activated 2-amino-2-methyl-1-propanol. *Chem. Eng. Sci.* **2009**, *64*, 1185–1194.
- (15) Zhu, D.; Fang, M.; Lv, Z.; Wang, Z.; Luo, Z. Selection of blended solvents for CO₂ absorption from coal-fired flue gas. Part 1: Monoethanolamine (MEA)-based solvents. *Energy Fuels* **2012**, *26*, 147–153.
- (16) Ume, B.C. S.; Ozturk, M. C.; Alper, E. Kinetics of CO₂ absorption by a blended aqueous amine solution. *Chem. Eng. Technol.* **2012**, *35*, 464–468.
- (17) Finkenrath, M. Carbon dioxide capture from power generation – Status of cost and performance. *Chem. Eng. Technol.* **2012**, *35*, 482–488.
- (18) Vinoba, M.; Bhagiyalakshmi, M.; Jeong, S. K.; Yoon, Y.; Nam, S. C. Immobilization of carbonic anhydrase on spherical SBA-15 for hydration and sequestration of CO₂. *Colloids Surf., B* **2012**, *90*, 91–96.
- (19) Mirjafari, P.; Asghari, K.; Mahinpey, N. Investigating the application of enzyme carbonic anhydrase for CO₂ sequestration purposes. *Ind. Eng. Chem. Res.* **2007**, *46*, 921–926.
- (20) Berg, J. M.; Tymoczko, J. L.; Stryer, L. *Biochemistry*, 6th ed., W.H. Freeman and Company: New York, 2007; pp 254–259.
- (21) Bond, G. M.; Stringer, J.; Brandvold, D. K.; Simsek, F. A.; Medina, M. G.; Egeland, G. Development of integrated system for biomimetic CO₂ sequestration using the enzyme carbonic anhydrase. *Energy Fuels* **2001**, *15*, 309–316.
- (22) Yan, M.; Liu, Z.; Lu, D.; Liu, Z. Fabrication of single carbonic anhydrase nanogel against denaturation and aggregation at high temperature. *Biomacromolecules* **2007**, *8*, 560–565.
- (23) Krishnamurthy, V. M.; Kauffman, G. K.; Urbach, A. R.; Gitlin, I.; Gudiksen, K. L.; Weibel, D. B.; Whitesides, G. M. Carbonic anhydrase as a model for biophysical and physical-organic studies of proteins and protein-ligand binding. *Chem. Rev.* **2008**, *108*, 946–1051.
- (24) Vinoba, M.; Bhagiyalakshmi, M.; Jeong, S. K.; Yoon, Y.; Nam, S. C. Carbonic anhydrase immobilized on encapsulated magnetic nanoparticles for CO₂ sequestration. *Chem.—Eur. J.* **2012**, *18*, 12028–12034.
- (25) Vinoba, M.; Bhagiyalakshmi, M.; Jeong, S. K.; Yoon, Y.; Nam, S. C. Capture and sequestration of CO₂ by human carbonic anhydrase covalently immobilized onto amine-functionalized SBA-15. *J. Phys. Chem. C* **2011**, *115*, 20209–20216.
- (26) Vinoba, M.; Lim, K. S.; Jeong, S. K.; Lee, S. H.; Alagar, M. Immobilization of human carbonic anhydrase on gold nanoparticles assembled onto amine/thiol-functionalized mesoporous SBA-15 for biomimetic sequestration of CO₂. *Langmuir* **2011**, *27*, 6227–6234.
- (27) Kim, Y. E.; Choi, J. H.; Nam, S. C.; Yoon, Y. CO₂ absorption characteristics in aqueous K₂CO₃/piperazine solution by NMR spectroscopy. *Ind. Eng. Chem. Res.* **2011**, *50*, 9306–9313.
- (28) Lim, J.; Kim, D. H.; Yoon, Y.; Jeong, S. K.; Park, K. T.; Nam, S. C. Absorption of CO₂ into aqueous potassium salt solutions of L-alanine and L-proline. *Energy Fuels* **2012**, *26*, 3910–3918.
- (29) Danckwerts, P. V. The reaction of CO₂ with ethanolamines. *Chem. Eng. Sci.* **1979**, *34*, 443–446.
- (30) Choi, S.; Dresse, J. H.; Jones, C. W. Adsorbent materials for carbon dioxide capture from large anthropogenic point sources. *ChemSusChem* **2009**, *2*, 796–854.
- (31) Xu, S.; Wang, Y. W.; Otto, F. D.; Mathe, A. E. Kinetics of the reaction of carbon dioxide with 2-amino-2-methyl-1-propanol solution. *Chem. Eng. Sci.* **1996**, *51*, 841–850.
- (32) McCann, N.; Phan, D.; Wang, X.; Conway, W.; Burns, R.; Attalla, M.; Puxty, G.; Maeder, M. Kinetics and mechanism of carbamate formation from CO₂(aq), carbonate species, and monoethanolamine in aqueous solution. *J. Phys. Chem. A* **2009**, *113*, 5022–5029.
- (33) Bottinger, W.; Maiwald, M.; Hasse, H. Online NMR spectroscopic study of species distribution in MEA–H₂O–CO₂ and DEA–H₂O–CO₂. *Fluid Phase Equilib.* **2003**, *263*, 131–143.
- (34) Barzaghi, F.; Mani, F.; Peruzzini, M. A ¹³C NMR investigation of CO₂ absorption and desorption in aqueous 2,2'-iminodiethanol and N-methyl-2,2'-iminodiethanol. *Int. J. Greenhouse Gas Control* **2011**, *5*, 448–456.
- (35) Ciftja, A. F.; Hartono, A.; da Silva, E. F.; Svendsen, H. F. Study on carbamate stability in the Amp/CO₂/H₂O system from ¹³C-NMR spectroscopy. *Energy Procedia* **2011**, *4*, 614–620.
- (36) Ramachandran, N.; Aboudheir, A.; Idem, R.; Tontiwachwuthikul, P. Kinetics of the absorption of CO₂ into mixed aqueous loaded solutions of monoethanolamine and methyldiethanolamine. *Ind. Eng. Chem. Res.* **2006**, *45*, 2608–2616.
- (37) Aboudheira, A.; Tontiwachwuthikula, P.; Chakmab, A.; Idema, R. Kinetics of the reactive absorption of carbon dioxide in high CO₂-loaded, concentrated aqueous monoethanolamine solutions. *Chem. Eng. Sci.* **2008**, *58*, 5195–5210.
- (38) Benamor, A.; Ali, B. S.; Aroua, M. K. Kinetic of CO₂ absorption and carbamate formation in aqueous solutions of diethanolamine. *Korean J. Chem. Eng.* **2008**, *25*, 451–460.
- (39) Teramoto, M.; Ohnishi, N.; Takeuchi, N.; Kitada, S.; Matsuyama, H.; Matsumiya, N.; Mano, H. Separation and enrichment of carbon dioxide by capillary membrane module with permeation of carrier solution. *Sep. Purif. Technol.* **2003**, *30*, 215–227.
- (40) Kanbar, B.; Ozdemir, E. Thermal stability of carbonic anhydrase immobilized within polyurethane foam. *Biotechnol. Prog.* **2010**, *26*, 1474–1480.
- (41) Sarraf, N. S.; Saboury, A. A.; Ranjbar, B.; Moosavi-Movahedi, A. A. Structural and functional changes of bovine carbonic anhydrase as a consequence of temperature. *Acta Biochim. Pol.* **2004**, *51*, 665–671.
- (42) Lavecchia, R.; Zugaro, M. Thermal denaturation of erythrocyte carbonic anhydrase. *FEBS Lett.* **1991**, *292*, 162–164.
- (43) Tourneux, D. L.; Iliuta, I.; Iliuta, M. C.; Fradette, S.; Larachi, F. Solubility of carbon dioxide in aqueous solutions of 2-amino-2-hydroxymethyl-1,3-propanediol. *Fluid Phase Equilib.* **2008**, *268*, 121–129.
- (44) Kernohan, J. C. The pH-activity curve of bovine carbonic anhydrase and its relationship to the inhibition of the enzyme by anions. *Biochim. Biophys. Acta* **1965**, *96*, 304–317.
- (45) Penders-van Elk, N. J. M. C.; Derk, P. W. J.; Fradette, S.; Versteeg, G. F. Kinetics of absorption of carbon dioxide in aqueous MDEA solutions with carbonic anhydrase at 298 K. *Int. J. Greenhouse Gas Control* **2012**, *9*, 385–392.
- (46) Nogent, H.; Tacon, X. L. The differential reaction calorimeter: A simple apparatus to determine reaction heat, heat transfer value and heat capacity. *J. Loss Prev. Process Ind.* **2002**, *15*, 445–448.
- (47) Nogent, H.; Tacon, X. L. The differential reaction calorimeter: Examples of use. *J. Loss. Prev. Process Ind.* **2003**, *16*, 133–139.

Supporting Information

Carbonic Anhydrase Promotes the Absorption Rate of CO₂ in Post-Combustion Processes

Mari Vinoba,[†] Margandan Bhagyalakshmi,[‡] Andrews Nirmala Grace^{†,‡} Dae Hoon

Kim,[†] Yeoil Yoon,[†] Sung Chan Nam,[†] II Hyun Baek,[†] Soon Kwan Jeong ^{†,*}

[†]*Korea Institute of Energy Research, Daejeon 305-343, Korea*

[‡] *CO₂ Research and Green Technologies Centre, VIT University, Vellore- 632014, India.*

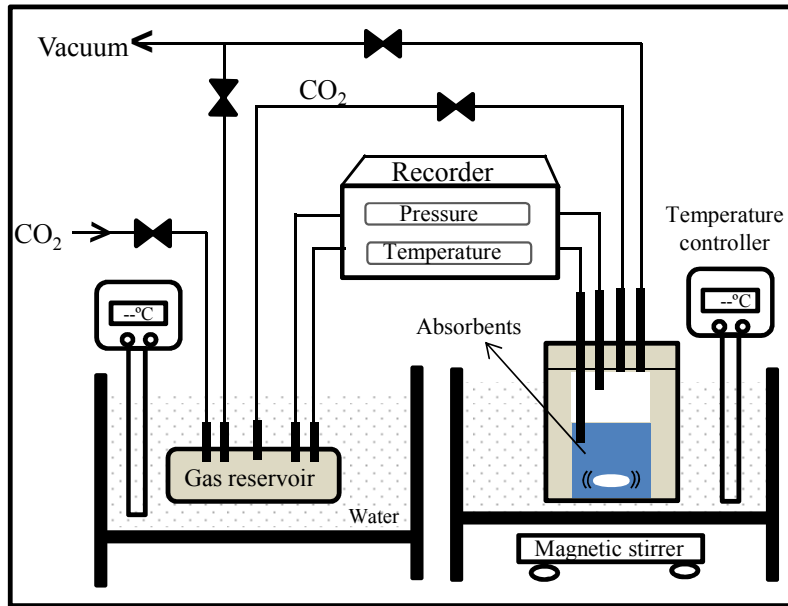


Figure S1. Schematic diagram showing the apparatus used to monitor the vapor–liquid equilibrium.

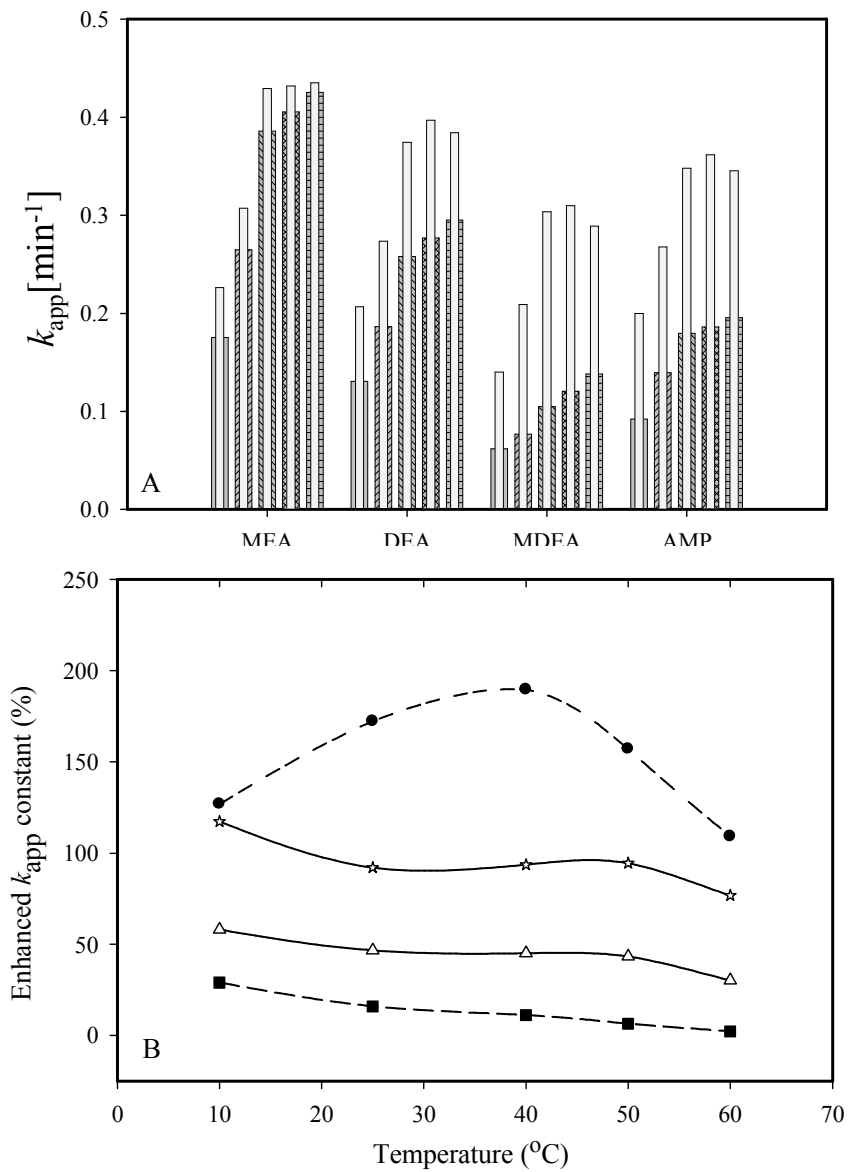


Figure S2. Optimization of the temperature that maximized the CO₂ absorption rate (A) and enhanced rate (B) by the presence of the CA enzyme in 10% of alkanolamines.

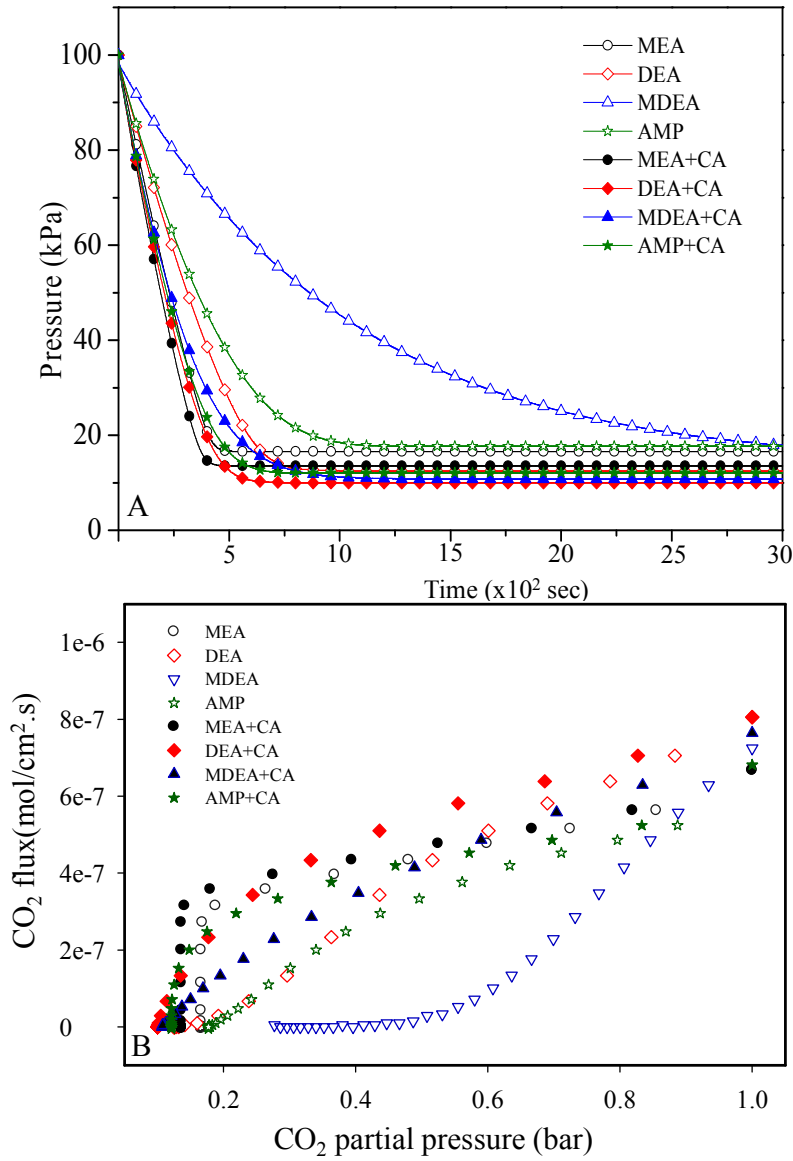


Figure S3. Reaction rates for the absorption of CO_2 by the 10% aqueous amine solutions at 40°C (A), and the CO_2 driving force for the gas–solvent system in the presence of the CA enzyme (B).

Table of Content (TOC) graphic

